SOLIDIFICATION IN TERNARY SYSTEMS

A. Aitta, H.E. Huppert, M.G. Worster
Inst. of Theoretical Geophysics, Dept. of Applied Mathematics and Theoretical Physics
University of Cambridge, Silver Street, Cambridge, CB3 9EW, U.K.
a.aitta@damtp.cam.ac.uk, heh1@esc.cam.ac.uk, mgw1@esc.cam.ac.uk

Keywords: ternary phase diagram, H_2O–KNO_3–$NaNO_3$, eutectic solid, cotectic mush, nucleation delay

Abstract The ternary solidification problem has been shown to reveal interesting fluid dynamical possibilities owing to fluid–density reversals that can appear during the solidification process. Proportions for the different solidified products are presented. Experimental results are obtained for the H_2O–KNO_3–$NaNO_3$ system when there is no fluid motion due to absence of both thermal and compositional convection. The growth rates for both one–component and two–component mushes as well as for the ternary solid are diffusion–limited. However, a substantial undercooling and a linear initial growth in time was measured for the ternary solid.

Introduction

Multicomponent solidification is a very common phenomenon both in nature and manufacturing. It occurs on a very big scale when magma solidifies to form rocks, and at precision scale in making modern materials or proteins. Generally, fluid flow is generated in the process and it influences both the structure and the properties of the solidified product. Binary systems are not sufficiently adequate to model all possible varieties of fluid flow. Three–component systems can reveal fundamentally new types of fluid flow. For example, the occurrence of internal fluid–density reversals could lead to still largely unknown flow phenomena. This paper gives the classification of the different flow regimes obtainable by cooling a system either from below or above and also the simplest estimates of the concentrations for the different solidified products. It reports the main experimental findings in the regime of no flow; a detailed description of the experimental set–up and measurements is discussed elsewhere (Aitta et al. (2001)). Our main conclusions are summarized in the final section.

1. TERNARY PHASE DIAGRAM

In order to understand three–component solidification one needs to construct a ternary phase diagram (West (1982)) incorporating three binary phase diagrams, one for each pair of components, on the (vertical) faces of a triangular prism. The vertical direction indicates increasing temperature, the horizontal directions changes in concentration. In a horizontal projection of the prism, as in figure 1, each corner represents a pure substance, and a binary eutectic point (e.g. E_{AB}) is on each side of the triangle. The extensions of the binary eutectic points into the interior of the triangle indicate the cotectic lines (where two components solidify simultaneously), and meet at the ternary eutectic point E where all three components crystallize at the same time if the temperature is lower than the eutectic temperature. For simplicity, solid solutions are assumed not to occur. The cotectic lines divide the space into three fields, each shown with a different shading. As long as the fluid concentration remains inside one field, cooling of the fluid below the liquidus temperature creates a mush, whose solid part consists of only the pure substance of the corner of the field. The fluid inside the solidified porous matrix is depleted of the solidified component and, if no convection occurs, during its subsequent solidification its concentration moves along the straight tie line in figure 1 going from the initial concentration of the fluid at O towards the cotectic line, with the extension of the tie line going through the corner A. When the residual fluid concentration reaches the cotectic line at P, two of the components crystallize simultaneously. Their ratio is given by where the tangent of the cotectic curve at P intercepts the AB edge. Then the residual fluid is depleted in both components A and B, and further solidification makes it follow the cotectic line towards the eutectic point if the temperature is low enough.

The ternary phase diagram can tell us some properties of the solidification product and of the fluid that we may expect. This is schematically shown in figure 2. Thermal equilibrium and no compositional convection are assumed. Compositional convection is avoided if component A is the lightest component. Thermal convection is avoided if the system is cooled at its bottom boundary, which is kept at a constant temperature T_{base}, and temperature increases upwards. At heights $z>h$, where $T>T_0$, there is only fluid. T_0 is the liquidus (saturation) temperature corresponding to the initial concentration of the fluid. When the temperature is below T_0 component A of the fluid starts to crystallize to form mush. Then the residual fluid is depleted of the component A and correspondingly enriched in the other components B and C at the

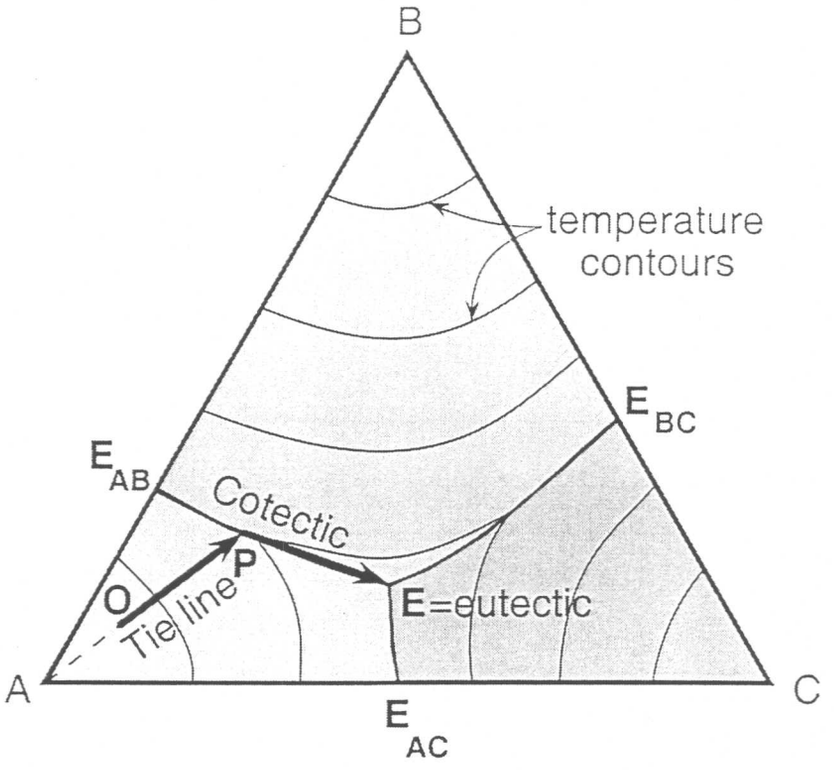

Figure 1 Ternary phase diagram. OPE is the liquid line of descent of the residual fluid when liquid with initial concentration O is progressively cooled below the eutectic temperature.

heights below h. At the height $z=h_C$ and temperature $T=T_P$, the second component B starts to solidify together with component A to form cotectic mush in the pores of the already crystallized A–mush. Below the height h_C the concentration of the component B (C_B) in the fluid starts to decrease as also does C_A, while C_C continues to increase but with a different slope. Below the eutectic temperature T_E, at the height $z=h_E$, the residual fluid in the pores of the cotectic mush is completely solidified into eutectic solid, which is forming in the eutectic ratio of the components. The solid below h_E has, overall, the components A, B and C in the same ratio as the initial fluid had them.

From the phase diagram one can calculate the fractions of the differently solidified components below h_E in terms of the initial fluid concentrations A_O, B_O, C_O and the eutectic concentration A_E, B_E, C_E. The fraction of eutectic solid is C_O/C_E, and the fraction of cotectic AB solid is $(B_O - C_O B_E/C_E)/B_t$, where B_t is approximately the fraction of B on the AB edge cut by the tangent at P to the cotectic curve. The rest is pure A.

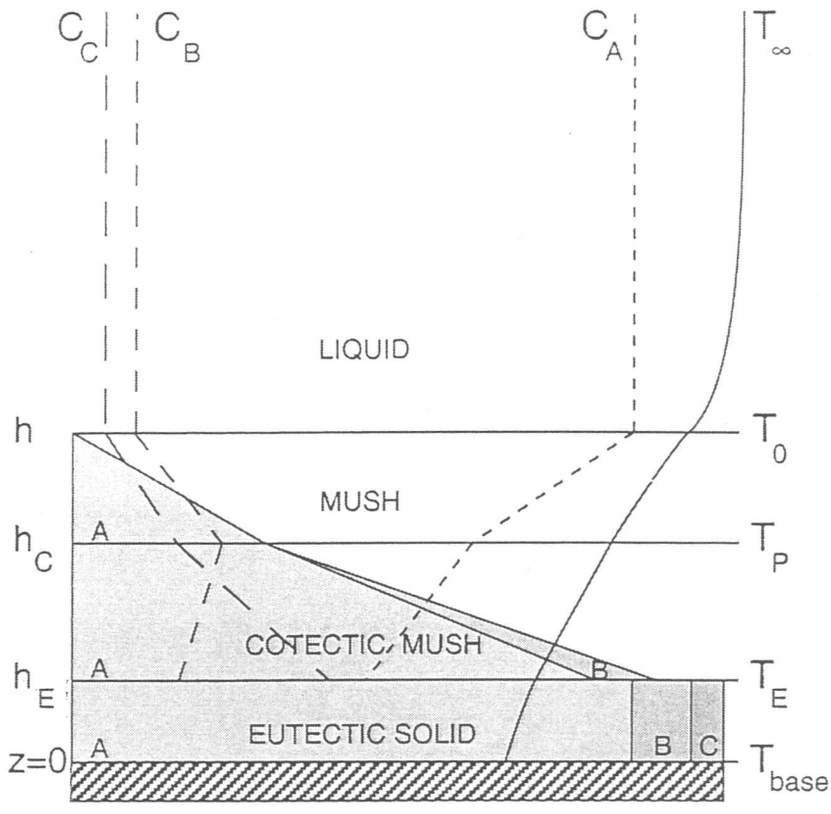

Figure 2 A schematic cross section during the solidification. The shaded area given to each component approximates linearly the proportion of each solidified product at different heights. The three dashed lines are the linearly estimated concentrations of the three components in the fluid. The solid curve indicates how the temperature is changing with depth.

Convection can arise in two possible ways. One can either change the cooling to be through the top boundary of the fluid which generates cooler heavier fluid above lighter warmer fluid leading to thermal convection; or, if the initial fluid concentration is not in the field of the lightest component, fluid flow is induced due to the compositional convection since the lighter residual fluid rises, as the heavier component solidifies. In order to classify the different types of flows a ternary phase diagram is drawn such that the fluid density increases from the bottom left hand corner towards the other corners and along the cotectic lines, as is shown by small arrows in figure 3. In each field there is a special tie line through the eutectic point. It divides the field so that all liquid lines of descent on one side go towards the cotectic line on that side, and hence chemically different cotectic mush is produced depending on which side the initial concentration lies. As shown in the table in the figure 3,

interesting and complicated interplays of fluid flows can be generated by choosing the regime of initial concentration and the cooling direction.

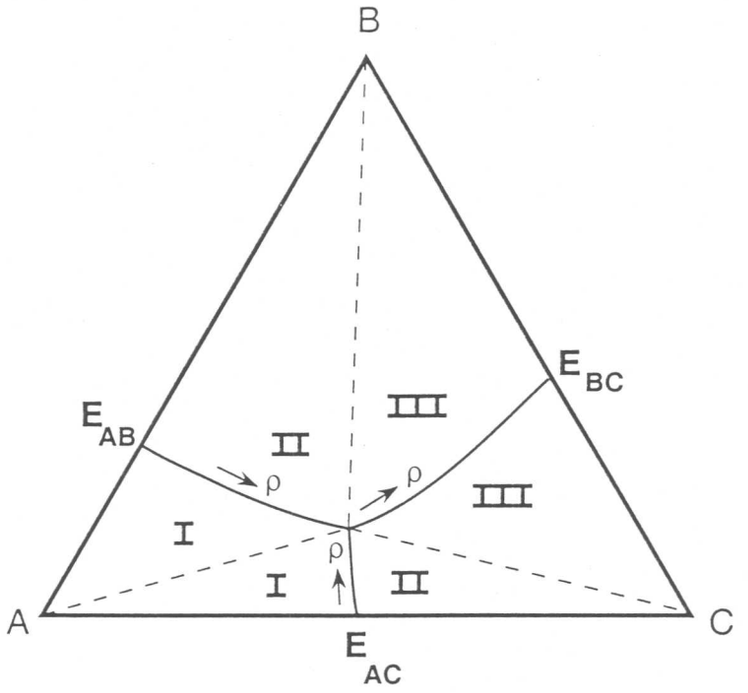

regime	crystallized component	fluid released	compositional convection	
			COOLED BELOW: NO THERMAL CONVECTION	COOLED ABOVE: ALWAYS THERMAL CONVECTION
I	A	heavy	no	yes
cotectic boundaries	A + B (or A + C)	heavy	no	yes
II	B	light	yes	no
cotectic boundaries	A + B (or A + C)	heavy	no	yes
III	B (or C)	light	yes	no
cotectic line	B + C	light	yes	no

Figure 3 Dynamically different regimes in a ternary system. Fluid density is assumed to change in the direction marked by arrows. The boundaries are either the cotectic lines or the tie lines to the eutectic point (dashed).

2. AN EXPERIMENTAL INVESTIGATION

For our studies we wanted to have a transparent liquid to allow visual observations, a simple phase diagram without unstable points or double salts in the regime of interest, the liquidus and eutectic temperatures accessible using simple laboratory coolers, and the concentrations to be readily measurable. We therefore chose H_2O–KNO_3–$NaNO_3$. Some of its saturation data were available in the literature (Linke (1965), Protsenko et al. (1971)), but the only values given below 0 °C were its binary and ternary eutectic points.

We used a transparent tank with movable insulating layers around it to allow visual measurements of the height of the growing mush and ternary solid. The base of the tank was kept at a constant temperature either close to or below the eutectic temperature. Thermistors were used to obtain a time–dependent record of the temperature of the base and at various heights in mush, solid and fluid. Samples were withdrawn from time to time at various heights and their salt concentrations were analyzed after suitable dilution using atomic absorption spectroscopy.

The location of the cotectic front was not visible to the eye. We were, however, able to estimate its height by using the concentration measurements, since the salt concentration in the residual fluid, as a function of height, changes from an increasing trend (for a one–component mush) to a decreasing trend (for a two–component mush where that salt is solidifying).

3. THE RESULTS

The growth of the one–component mush (ice), two–component mush (ice + KNO_3) and the eutectic solid is shown in figure 4a. After the initial, more rapid growth, their heights are growing proportional to the square root of time. This type of power law is expected in diffusion–limited growth (Huppert & Worster (1985)). The growth of the ice mush slows down after a day or so owing to the finite height of the container. The long nucleation delay (2.8 h) for the eutectic solid and its linear initial growth in time (during the next 4 h) as shown in figure 4b was quantitatively measured for a ternary solid, for the first time to our knowledge.

From the salt concentrations as a function of temperature (available for each sampling height from the temperature profile measurements) we noticed a substantial undercooling occurring before the initiation of both the cotectic mush and ternary–solid crystallization.

By representing the concentration profiles at various times for both salts one finds that the KNO_3 concentration is constant above the mush,

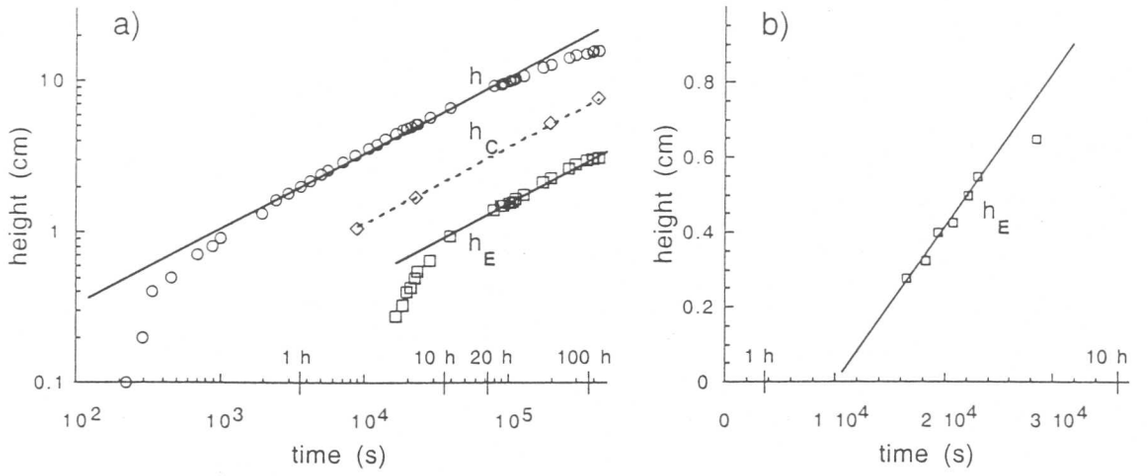

Figure 4 Measured height of the ice–mush and the eutectic solid, and deduced height of the cotectic mush: a) logarithmic scale, b) early stages of the eutectic solid growth in a linear scale.

increases at first with the depth of the mush, but at greater depths decreases again as shown in figure 5. The increase is due to the formation of ice mush, and the decrease at the greater depths is due to the formation of cotectic mush made of KNO_3 and ice. The turning points in the concentration profiles have been used to estimate the heights of the cotectic mushes at various times as shown in figure 4. Similar turning points were not present in the corresponding $NaNO_3$ concentration profiles.

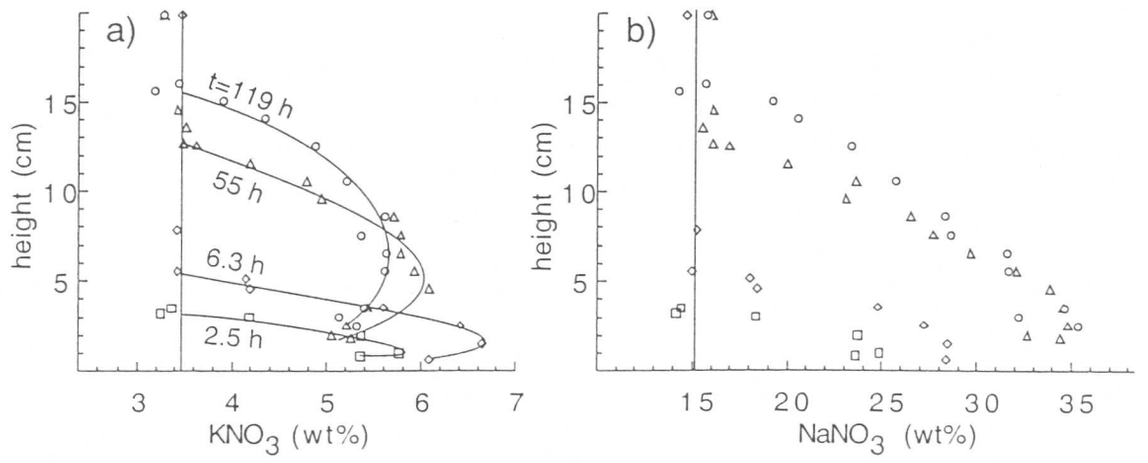

Figure 5 Salt concentration profiles at various times.

The evolution of the fluid concentration is shown in figure 6, using a different symbol for each of seven experiments. The initial concentration is marked by a solid circle and the previously published (Linke (1965), Protsenko et al. (1971)) binary and ternary eutectic points by solid squares. Lines through the origin and the initial concentration points are the tie lines. The data follow them most of the time. However, the data do not reach the straight lines connecting the binary and ternary eutectic points. For this reason we have given new estimates for the cotectic lines, hand drawn using the data. The thin line is drawn through the eutectic points. The thicker line is drawn without this restriction, and we believe it is a more reliable indicator of the cotectic line for this system.

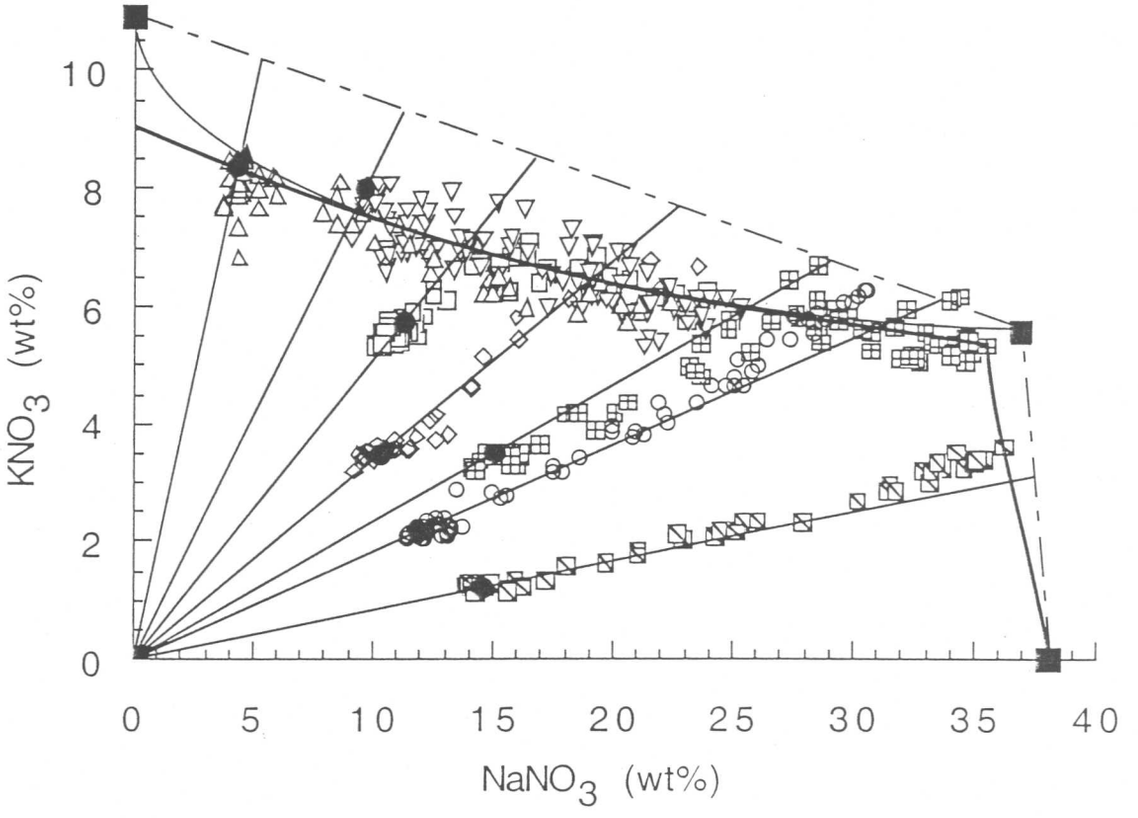

Figure 6 Descent paths for various experiments allows one to estimate the locations of the cotectic lines.

4. SUMMARY

A classification of the possible fluid flows has been obtained. The ternary phase diagram is divided into three regimes where not only the solidification products but also the generated fluid flows are different. In addition, the nature of the fluid flow is influenced by whether the cooling direction is from below or above. In particular, flow can arise or diminish while the solidification is proceeding due to the change of the direction in the concentration gradients.

In the simplest case there is no fluid flow due to the absence of both thermal and compositional convection. Then one can calculate the proportions of the different solidification products.

Experimental results have been obtained for this case where there is no convection: cooling is induced from below and the initial concentration of salts was in the regime where the solidification releases heavy fluid.

Both the single component mush and the cotectic mush as well as the eutectic solid have diffusion controlled growth; they all grow proportionally to the square root of time.

The eutectic solid has a significant nucleation delay and initially a linear growth in time.

The slope of the concentration profile of one of the ternary components can change from positive to negative during the solidification. This made it possible to determine the height of the invisible cotectic mushy layer.

The concentration evolution of the residual liquid, called the liquid line of descent, was obtained for seven experiments with different initial concentrations. They followed well the tie lines and then the cotectic line, as is to be expected for systems in thermal equilibrium.

Estimates for the two cotectic salt–ice lines in the phase diagram were obtained. Both of them differ somewhat from what one can linearly approximate using the only previously available data, namely the binary and ternary eutectic point concentrations given in the literature. The longer cotectic line shows a curvature not previously evaluated. So we now have a much more detailed knowledge of the phase diagram for the potassium nitrate – sodium nitrate – water ternary system.

Substantial undercooling was found for both cotectic mush and eutectic solid, not previously noticed in ternary systems. They show a non–equilibrium aspect of this process.

Acknowledgments

During the main part of this work A.A. had a Daphne Jackson Fellowship supported by Lucy Cavendish College, University of Cambridge and The Thriplow Char-

itable Trust. A.A. also obtained a Euromech Fellowship and a travel grant from the Royal Society to participate in this conference.

References

Aitta, A., Huppert, H.E., Worster, M.G. Diffusion–controlled solidification of a ternary melt from a cooled boundary, *Journal of Fluid Mechanics* **432** (2001) 201–217.

Huppert, H.E., Worster, M.G. Dynamic solidification of a binary melt, *Nature* **314** (1985) 703–707.

Linke, W.F. *Solubilities of inorganic and metal–organic compounds. Volume II* 4th edition, American Chemical Society, Washington D.C. (1965).

Protsenko, P.I., Razumovskaya, O.N., Brykova, N.A. *Spravochnik po rastvorimosti nitritnykh i nitratnykh solevykh sistem*, ed. Zdanovskii, A.B., Leningrad: Khimiya, (1971).

West, D.R.F. *Ternary Equilibrium Diagrams* (2nd edition), Chapman and Hall, London, (1982).